Annals of Nuclear Medicine Vol. 16, No. 1, 25–32, 2002

Myocardial viability assessment with gated SPECT Tc-99m tetrofosmin % wall thickening: Comparison with F-18 FDG-PET

Atsushi MARUYAMA,* Shinji HASEGAWA,* Asit Kr. PAUL,* Mu XIULI,* Jun YOSHIOKA,* Kaoru MARUYAMA,* Masatsugu HORI** and Tsunehiko NISHIMURA*

**Division of Tracer Kinetics, and **Department of Internal Medicine and Therapeutics, Osaka University, Graduate School of Medicine*

Object: This study was designed to assess the value of gated SPECT Tc-99m-tetrofosmin (TF) wall thickening (WT) in addition to TF exercise (Ex)/rest myocardial SPECT, in comparison with F-18 fluorodeoxyglucose (FDG)-PET. ***Methods:*** The study population consisted of 33 patients with old myocardial infarction (27 men and 6 women; mean age, 62 ± 8 years old). All patients underwent Ex/rest TF SPECT and glucose loading FDG-PET. Polar map images of Ex/rest TF were generated and divided into 24 segments for further analysis. We classified LV segments according to the exercise-rest perfusion scintigraphy. LV segments with less than 70% of the maximum TF activity on the exercise image were defined as stress-induced defects. Among these, the segments whose TF activity increased by 10% from exercise to rest images or exceeded 70% of the maximum uptake were defined as reversible (viable) defects. The remaining defects on the rest image were irreversible (non-viable) defect segments, and were considered for viability study on the basis of %WT. %WT was calculated according to the standard method: {(counts ES – counts ED)/counts ED} × 100. A viable segment on gated SPECT was defined as a segment whose %WT exceeded the lower limit of the normal value (mean – SD). PET viability was defined as FDG uptake exceeding 50% of the maximum count. ***Results:*** Among the 792 segments evaluated in the 33 patients studied, there were 689 PET viable segments. Of the 689 segments analyzed, 198 (29%) were identified as having defects on Ex images. Among these defects, 55 (8%) were reversible or partially reversible, as evidenced by rest images, and 143 (21%) were irreversible. Of the irreversible segments on Ex/rest images, 106 (15%) demonstrated no apparent WT by gated TF SPECT, whereas 37 (6%) segments with irreversible defects did have apparent WT. Overall, the sensitivity of Ex/rest TF perfusion imaging was 79%. Sensitivity was improved from 79% to 85% by combining %WT and perfusion data, but specificity was reduced from 70% to 56%. ***Conclusion:*** %WT evaluated from gated TF imaging enhanced myocardial viability assessment in comparison with FDG-PET.

Key words: myocardial viability assessment, gated SPECT, wall thickening, FDG-PET

INTRODUCTION

ELECTROCARDIOGRAPHIC (ECG) gated acquisition of technetium 99m (Tc-99m)-labeled flow tracers single-photon emission computed tomography (SPECT) offers the possibility of simultaneously assessing myocardial perfusion and left ventricular function within a single study, and fast microcomputers have made gated SPECT available as a routine clinical study.[1] In addition to left ventricular function (global ejection fraction) as an important determinant of prognosis in patients with coronary artery disease (CAD), regional wall thickening (WT) has been shown to be an important parameter as it may indicate viable myocardium.[2] Tc-99m-tetrofosmin (TF) is a cationic diphosphine which compares well with Tl-201 in

Received June 28, 2001, revision accepted October 1, 2001.

For reprint contact: Tsunehiko Nishimura, M.D., Ph.D., Division of Tracer Kinetics, Osaka University, Graduate School of Medicine (D9), 2–2, Yamada-oka, Suita, Osaka 565–0871, JAPAN.

E-mail: nisimura@tracer.med.osaka-u.ac.jp

the assessment of myocardial perfusion, and it has been used in evaluating left ventricular function as described above.[3,4]

In contrast, F-18 fluorodeoxyglucose (FDG)-PET has been shown to identify viable tissue in ischemic myocardium.[5–9] Glucose metabolism assessed by loading FDG-PET was demonstrated to be preserved in some areas of resting perfusion defect by Tc-99m-labeled flow tracers in CAD patients. Therefore, the use of Tc-99m-labeled flow tracers at rest underestimates the extent of viable myocardium in CAD.[10,11] Furthermore, it was demonstrated that visual (semiquantitative) analysis of resting WT by means of ECG-gated SPECT Tc-99m myocardial imaging accurately predicts the reversibility of stress-induced perfusion defects.[12] Nevertheless, the relationships among the amount of regional myocardial TF uptake, myocardial WT and myocardial viability as assessed by metabolic PET imaging have not yet been elucidated. This study was therefore undertaken to assess the additional value of gated SPECT Tc-99m TF WT in addition to TF exercise (Ex)/rest myocardial SPECT, in comparison with FDG-PET.

MATERIALS AND METHODS

Study population

Thirty-three patients (27 male and 6 female; mean age, 62 ± 8 years) were included in this study. They had historic or ECG evidence of previous myocardial infarction and angiographically proven CAD. There were 13 patients with single-vessel, 12 with two-vessel and 8 with triple-vessel disease. All patients underwent ECG-gated technetium-99m TF Ex/rest SPECT and FDG-PET. ECG-gated SPECT, and FDG-PET studies were performed within 7 days. Exclusion criteria included left bundle branch block, unstable angina and recent myocardial infarction (within 4 weeks prior to the studies).

Technetium-99m tetrofosmin myocardial SPECT

After an overnight fast, each patient underwent an exercise stress protocol based on clinical status. At an appropriate symptom-limited treadmill end-point (chest pain, shortness of breath, significant ST-T change, blood-pressure depression and leg fatigue at an adequate workload), 370 MBq of Tc-99m TF (Myoview, Nihon Medi-Phisics, Tokyo, Japan) was injected, followed by flushing with 20 m*l* of saline. After intravenous injection, patients were given 200 m*l* of whole milk to increase biliary elimination. ECG-gated myocardial SPECT was performed 1 hour after administration. SPECT imaging was performed with a triple-headed rotating gamma camera [GCA9300A/HG, Toshiba Medical Co., Tokyo, Japan].[13] Full-width at half-maximum (FWHM) of this camera was about 10 mm. Acquisition parameters were as follows: matrix 64 × 64 (pixel size 6.4 mm), triple-head with clockwise rotations of 120 degrees each (total 360 degrees), 20 views per head and 90,000 ms/view resulting in an acquisition time of 35 min. Gating was performed with 10 frames per R-R interval in the ECG. R-R interval allowable change was 20%.

At 1.5 hours after completion of the exercise image acquisition, the patients were injected with 740 MBq of Tc-99m TF followed by flushing with 20 m*l* of saline. SPECT imaging was subsequently performed 1 hour after the resting administration according to the SPECT acquisition protocol as described above. The raw Tc-99m TF data from the stress and rest acquisition were reconstructed by using a Butterworth filter with a 0.28 cycle/pixel cut-off.

F-18 fluorodeoxyglucose PET

After an overnight fast, attenuation corrected, ungated PET scans were obtained with a whole-body PET camera (SET-2400W [Headtome V], Shimadzu Medical Co., Kyoto, Japan) with a field-of-view of 590 mm within 7

No. of segment	Mean ± SD	No. of segment	Mean ± SD
1	30.5 ± 8.4	13	32.4 ± 9.7
2	33.6 ± 9.7	14	37.1 ± 9.1
3	45.3 ± 13.2	15	49.3 ± 12.3
4	32.8 ± 8.4	16	28.7 ± 10.0
5	34.9 ± 8.8	17	31.6 ± 9.8
6	47.3 ± 12.7	18	42.5 ± 11.0
7	43.1 ± 19.8	19	26.1 ± 8.0
8	39.7 ± 12.3	20	30.8 ± 9.3
9	49.7 ± 12.8	21	42.1 ± 13.4
10	38.7 ± 13.7	22	28.3 ± 10.0
11	38.7 ± 12.5	23	35.5 ± 11.0
12	51.9 ± 13.6	24	46.1 ± 14.2

Fig. 1 *Left*, polar maps of the left ventricular wall from the apex to the base divided into 24 segments: 3 short-axis slices from the apical, middle and basal ventricular levels divided into 8 segments. *Right*, table showing normal values (Mean ± SD) of % wall thickening in each of the 24 segments.

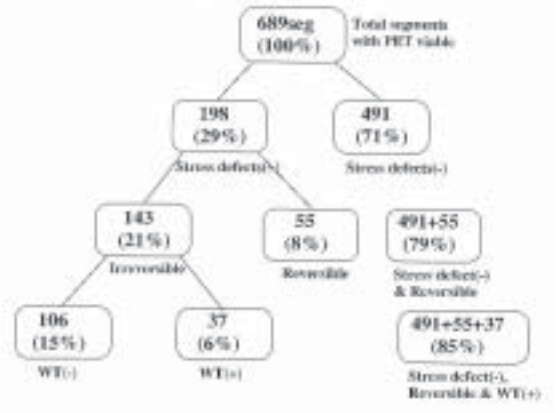

Fig. 2 Flow diagram depicting the presence or absence of stress defect reversibility on analysis of Ex/rest summed SPECT Tc-99m TF image pairs, and the prevalence of quantitative regional wall thickening on analysis of gated images for each category of irreversible defect. WT, Wall thickening. (%), Percentage of total PET-viable segments.

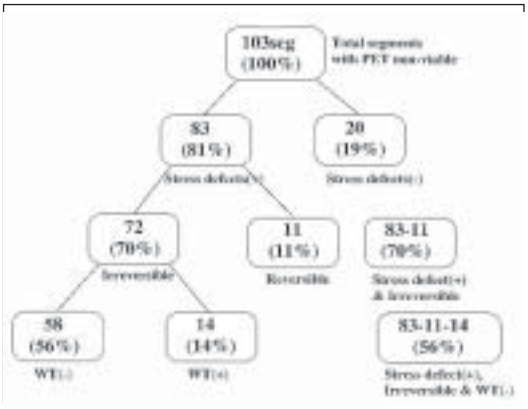

Fig. 3 Flow diagram depicting the presence or absence of stress defect reversibility on analysis of Ex/rest summed SPECT Tc-99m TF image pairs, and the prevalence of quantitative regional wall thickening on analysis of gated images for each category of irreversible defect. WT, Wall thickening. (%), Percentage of total PET non-viable segments.

days before or after SPECT imaging. The camera had a resolution of about 4 mm FWHM. Attenuation correction was performed by measuring a transmission scan with a germanium-68 ring source. One block ring configuration provides 63 transaxial image planes over 20 cm in axial width, and each slice width was 3.125 mm. Sixty minutes before injection of approximately 370 MBq of FDG, the patients received 75 g of glucose orally over 30 mins, and were then given lunch. Ten-minute emission scans were then acquired. PET scans were reconstructed by means of a Ramp and Butterworth convolution filter with a cut-off frequency of 0.0625 cycle/mm and a defined zoom factor. To obtain the same in-plane pixel size as the SPECT imagings (6.4 × 6.4 mm), two PET slices were added to obtain a comparable axial pixel size for PET (6.25 × 6.25 mm) and SPECT (6.4 × 6.4 mm).

Quantitative analysis of myocardial PET and SPECT

All patients underwent Ex/rest TF gated SPECT and glucose loading FDG-PET. In each patient, polar maps of Ex/rest TF were generated and divided into 24 segments for further analysis: 3 short-axis slices from the apical, middle and basal ventricular levels were chosen. The basal and middle ventricular short slices were divided into 8 segments, and the apical ventricular short-axis slice was also divided into 8 segments (Fig. 1).

For analysis of Ex/rest TF uptake, the frames of the raw tomographic data were summed and non-gated tomograms were reconstructed. TF uptake on summed images was calculated and expressed as % of maximum uptake. %WT (% wall thickening) was calculated according to the standard method: {(counts ES – counts ED)/counts ED} × 100. A polar map of FDG-PET was generated and also divided into 24 segments, as described above.

Definition of myocardial viability

We classified LV segments according to the exercise-rest perfusion scintigraphy. LV segments with less than 70% of the maximum TF activity on the exercise image were defined as stress-induced defects. Among these, the segments whose TF activity increased by 10% from exercise to rest images or exceeded 70% of the maximum uptake on the rest image were defined as viable defects.[14,15] The remaining defects were non-viable defect segments, and were considered for viability study on the basis of %WT. A viable segment on gated SPECT was defined as a segment whose %WT exceeded the lower limit of the normal value (mean – SD), which was estimated from 20 age and gender matched healthy persons. PET viability was defined as FDG uptake exceeding 50% of the maximum count.[10,11,16]

Statistical analysis

Mean values of continuous variables were compared by means of an unpaired t-test. A value of $p < 0.05$ was accepted as the minimal level of significance. Sensitivity, specificity, positive predictive values and negative predictive values were calculated in the standard fashion, considering FDG-PET as a gold standard.

RESULTS

Among the 792 segments evaluated in the 33 patients studied, there were 689 PET viable segments and 103 PET non-viable segments. The results for the Ex/rest imaging and the corresponding WT data from the gated SPECT TF images are presented in Figure 2 and Figure 3.

Of the 689 PET viable segments analyzed, 491 (71%) segments were identified as viable and 198 (29%) as defects on Ex images. As to the defects, 55 (8%) of 689

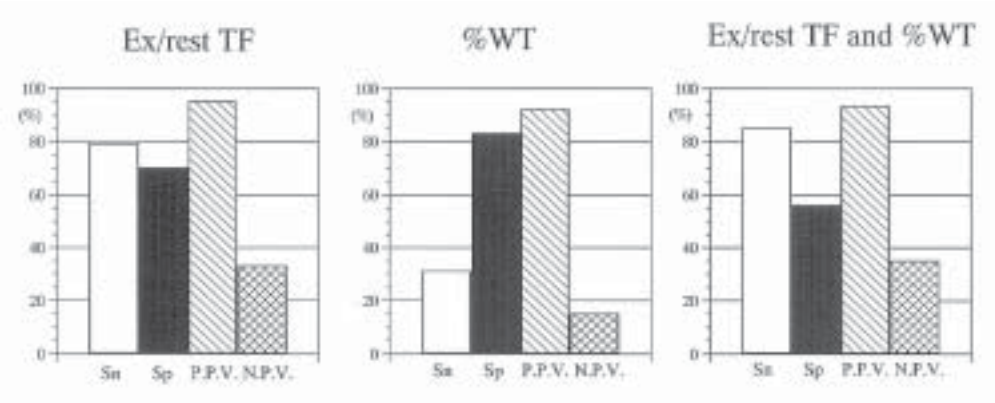

Fig. 4 Myocardial viability assessment by Ex/rest TF SPECT: FDG-PET was defined as the gold standard for myocardial viability; sensitivity (Sn), specificity (Sp), positive predictive value (P.P.V.) and negative predictive value (N.P.V.).

segments were reversible or partially reversible defects, as shown by rest images, and 143 (21%) were irreversible. Of the 143 irreversible defects on Ex/rest images, 106 (15%) demonstrated no apparent WT on gated TF imaging; 37 (6%) of the irreversible defects demonstrated apparent WT. Overall, the sensitivity of Ex/rest TF perfusion imaging was 79%. Sensitivity was improved from 79% to 85% by combining %WT and perfusion data (Fig. 2).

On the other hand, of the 103 PET non-viable segments analyzed, 83 (81%) were identified as having defects on Ex images. Among these defects, 11 (11%) were reversible or partially reversible, as evidenced by rest images, and 72 (70%) were irreversible. Of the irreversible segments on Ex/rest images, 14 (14%) demonstrated apparent WT on gated TF SPECT, whereas 58 (56%) segments with irreversible defects had no apparent WT. Overall, the specificity of Ex/rest TF perfusion imaging was 70%. Specificity was reduced from 70% to 56% when %WT and perfusion data were combined (Fig. 3). The sensitivity and specificity of %WT alone were 31% and 83%, respectively (Fig. 4).

Case 1 (Fig. 5) was a 72-year-old female suffering from anterior myocardial infarction. Percent uptake of TF in the antero-septal region on an Ex image was less than 70%. There was no increase in antero-septal TF activity in the rest image as compared to the Ex image, but WT was preserved in the antero-septal region. Furthermore, the antero-septal region was also viable on the FDG image. In this case, viable myocardium was underestimated by Ex/rest TF as compared to FDG-PET, but %WT showed additional value in the viability assessment.

Case 2 (Fig. 6) was a 67-year-old male suffering from posterior myocardial infarction. Percent uptake of TF in the postero-lateral region on an Ex image was less than 70%. There was no increase in postero-lateral TF activity in the rest image as compared to the Ex image. WT was not preserved in the postero-lateral region. The postero-lateral region was non-viable on the FDG image. Non-viable myocardium was assessed by Ex/rest TF and additional %WT, for comparison with FDG-PET.

DISCUSSION

Our data demonstrate that when wall thickening is apparent on gated SPECT imaging within the region of an Ex/rest perfusion defect, this finding is associated with reversibility of the stress defect on the rest image in comparison with FDG-PET. Sensitivity improved from 79% to 85% when %WT and perfusion data were combined.

Several authors have used quantitative and semi-quantitative analysis of WT on gated Tc-99m sestamibi images to assess viability, as a means of predicting Ex defect reversibility. Ziffer et al.[17] used quantitative analysis and obtained results similar to those of the current study, demonstrating that regional systolic WT in the region of an Ex defect can predict the defect on a rest image. Snapper et al.[12] and Chua et al.,[18] employing rest Tc-99m sestamibi and Tl imaging respectively, used semi-quantitative visual analysis and found that the presence of visually apparent WT on gated Tc-99m sestamibi imaging correlated with stress defect reversibility.

As in our group of patients with proven CAD, Williams et al.[19] demonstrated high sensitivity but modest specificity and positive predictive value with quantitative analysis of gated SPECT WT as a means of predicting rest reversibility of severe stress defects. As our data and those of others[12,18,20] have demonstrated, the correlation of WT data with stress defect reversibility may be less than optimal in patients with CAD or stress defects of severe magnitude.

Gated SPECT imaging has been validated by comparison with echocardiography[18,21,22] and cine MRI.[23,24] Tischler et al.[22] found much better agreement between gated planar sestamibi imaging and echocardiography, while Chua et al.[18] and Anagnostopoulos et al.[23] found that in well-perfused segments gated sestamibi SPECT

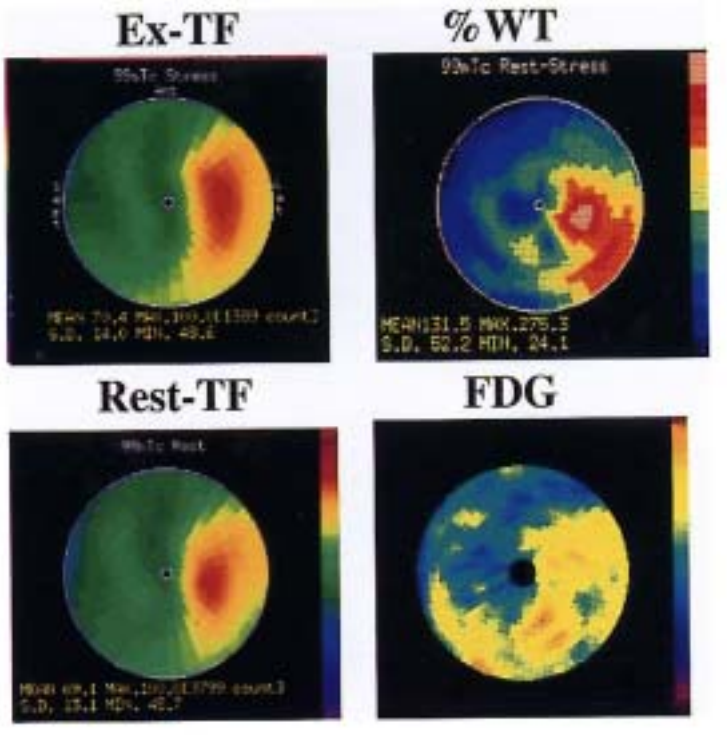

Fig. 5 A 72-year-old female patient with previous anterior wall myocardial infarction (see text). *Left*, polar map of % uptake of Ex/rest TF. *Right upper*, polar map of %WT. *Right lower*, polar map of % uptake of FDG.

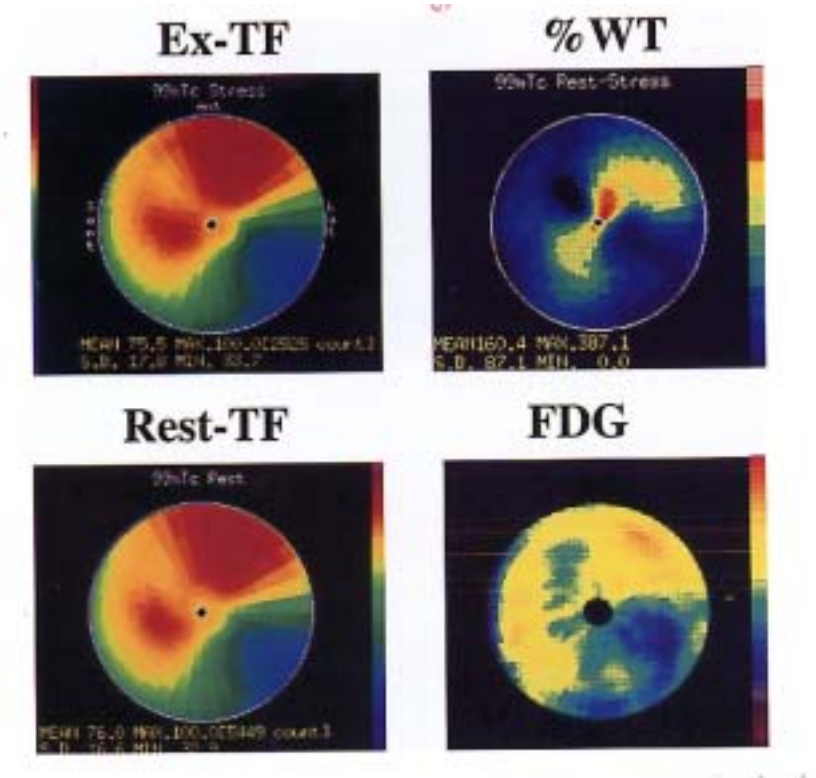

Fig. 6 A 67-year-old male patient with previous posterior wall myocardial infarction (see text). *Left*, polar map of % uptake of Ex/rest TF. *Right upper*, polar map of %WT. *Right lower*, polar map of % uptake of FDG.

results agreed well with those of echocardiography and MRI, respectively. Furthermore, Stollfuss et al.[25] demonstrated that gated SPECT provided reliable estimates of regional WT and global function in patients with low angiographic LVEF. Gunning et al.[24] found gated Tc-99m TF imaging to provide an accurate assessment of myocardial wall motion and thickening.

Although previous studies demonstrated WT to play an important role in myocardial viability assessment, the normal range of %WT has not been precisely evaluated.[2,12,17–26] Therefore, in our study, 20 age and gender matched volunteers underwent gated TF SPECT, and we calculated the normal range of %WT for each segment as previously described. The normal value for each segment varied from 26.1 ± 8.0% (basal septal, segment 19 of Fig. 1) to 51.9 ± 13.6% (apex, segment 12). We defined an apparent WT segment (viable segment) by gated TF as a segment with a value exceeding the normal value (mean – 1 SD).

Myocardial FDG uptake has been accepted as a means of noninvasively estimating myocardial viability in ischemic heart disease[5,6,27–34] and has been shown to be a predictor of outcome in bypass surgery patients.[5,6] Altehoefer et al.[10,11] demonstrated that segments could be categorized as PET viable (corresponding F-18 FDG uptake > 70%), PET non-viable (FDG uptake < 50%) and "intermediate" (FDG uptake 50%–70%). "Intermediate" FDG uptake may represent a mixture of viable and necrotic myocardium. One histopathologic study showed a wide range of areas with muscle loss and fibrosis in portions of the myocardium with wall motion abnormalities, and the percentage of muscle loss varied between <10% and >75%, indicating a wide range of myocardial damage in patients with CAD.[16] Therefore, in our study, PET viability was defined as FDG uptake exceeding 50% of that in the normal region.

We therefore considered FDG-PET to be the gold standard for assessing myocardial viability and compared this method with the combination of perfusion imaging and WT in the same patient group. This is the first study to use quantitative analysis of WT on gated TF in reference to FDG-PET. Nevertheless, additional assessment of %WT by TF myocardial gated SPECT improved the estimation of myocardial viability, which is generally underestimated by TF Ex/rest myocardial SPECT, as compared with FDG-PET. Sensitivity improved from 79% to 85% when %WT and perfusion data were combined.

On the other hand, specificity was reduced from 70% to 56% when %WT and perfusion data were combined. The decrease in specificity might be explained as follows. Although we defined %WT as {(counts ES – counts ED)/ counts ED} × 100, this formula is actually the percent count increase (%CI). As to current understanding of the relationship between wall thickening and count increase, Hoffman et al. showed, that for an object smaller than the resolution of the imaging system, the reconstructed count density is related to the size of the object,[35] that is, due to partial volume effect, the ED count in the region of the thin myocardium is apt to be underestimated, resulting in an overestimation of %CI, which was taken as a measure of %WT in the present study. This overestimation of myocardial viability might cause the decrease in specificity. But one study showed, in ECG-gated SPECT, that the %CI was a reliable index of wall thickness because the values for baseline myocardial thickness were generally up to 10 mm in normal subjects.[36]

Technical limitations of direct SPECT and PET comparisons are due to inherent differences in tomographic systems with and without attenuation correction.[10,11,37] PET data are corrected for photon attenuation, but SPECT data are not. Nevertheless, the myocardial SPECT imaging method is well established as a means of viability evaluation in ischemic heart disease despite photon attenuation. In a comparison of the quantification of SPECT and PET, no attenuation correction for SPECT need be taken into consideration for SPECT and PET uptake ratios in regard to myocardial viability from scar to ischemic tissues. Uptake ratios vary among anatomical areas and according to myocardial viability. In addition, uptake ratios are influenced by the partial volume effect. The underestimation of true tracer activity increases as WT increases and depends on the spatial resolution,[37] which is different for SPECT and PET. FWHM of this SPECT system was two and a half times as wide as that of this PET system, as described above.

Nevertheless, we have used very similar slice thickness for SPECT and PET, 6.4 mm and 6.25 mm, respectively. These thicknesses are also accepted for adequate comparison, as Altehoefer et al.[10,11] used slice thicknesses of 6.25 mm for SPECT and 6.75 mm for PET.

Many previous studies used a 50% threshold for myocardial viability,[11,38–40] but we used a 70% threshold for normal activity based on previous studies as follows.[14,15] Cuocolo et al.[14] indicated that in patients with chronic myocardial infarction and impaired LV function, quantitative analysis of Tl-201 and MIBI SPECT activity at rest predicts recovery of regional and global ventricular dysfunction after revascularization, and when all dysfunction segments were considered, the best cutoff point in the identification of reversible LV dysfunction for both Tl-201 and MIBI SPECT activity was 67%. Udelson et al.,[15] with a threshold of 60%, also suggested that quantitative analysis of regional activities of both Tl-201 and MIBI after rest injection can differentiate viable from non-viable myocardium in patients with coronary artery disease.

There are also certain limitations in differentiating between attenuation artifacts and true regional infarction. The presence of visual apparent WT on gated SPECT Tc-99m MIBI imaging, in a segment with an irreversible stress defect, reportedly assists in differentiating attenuation artifacts from true regional infarction.[41] In another

study,[12] however, the finding of an irreversible defect on stress and rest imaging with preserved WT by ECG-gated imaging was uncommon, occurring in <1% of all segments studied and <3% of all segments with stress-associated defects. In our investigation, however, such defects were seen in 4.7% of all 792 segments studied and in 19% of stress defects (Fig. 2). The prevalence of this kind of abnormality will be affected by the population studied, that is, this finding would be expected more often among obese and large-breasted subjects.

CONCLUSIONS

In conclusion, additional assessment of % wall thickening by Tc-99m TF myocardial gated SPECT improved estimation of myocardial viability, which is usually underestimated by TF Ex/rest myocardial SPECT, in comparison with FDG-PET. The major advantage of our study is that we used matched tomographic planes, allowing comparative quantitative evaluation of FDG-PET, Ex/rest regional perfusion imaging by Tc-99m TF SPECT and regional %WT as assessed with gated SPECT. Our approach is useful for assessing myocardial viability in patients with CAD and reduces the underestimation of myocardial viability which is a limitation of TF myocardial gated SPECT.

REFERENCES

1. Faber TL, Akers MS, Peshock RM, Corbett JR. Three-dimensional motion and perfusion quantification in gated single-photon emission computed tomograms. *J Nucl Med* 1991; 32: 2311–2317.
2. Perrone-Filardi P, Bacharach SL, Dilsizian V, Maurea S, Frank JA, Bonow RO. Regional left ventricular wall thickening. Relation to regional uptake of F-18 FDG-PET and Tl-201 TlCl in patients with chronic coronary artery disease and left ventricular dysfunction. *Circulation* 1992; 86: 1125–1137.
3. Tamaki N, Takahashi N, Kawamoto M, Torizuka T, Tadamura E, Yonekura Y, et al. Myocardial tomography using technetium-99m-tetrofosmin to evaluate coronary artery disease. *J Nucl Med* 1994; 35: 594–600.
4. Zaret BL, Rigo P, Wackers FJ, Hendel RC, Braat SH, Iskandrian AS, et al. Myocardial perfusion imaging with technetium-99m-tetrofosmin: comparison to Tl-201 imaging and coronary angiography in a phase III multicenter trial. *Circulation* 1995; 91: 313–319.
5. Tillisch J, Brunken R, Marshall R, Schwaiger M, Mandelkern M, Phelps M, et al. Reversibility of cardiac wall motion abnormalities predicted by positron tomography. *N Engl J Med* 1986; 314: 884–888.
6. Tamaki N, Yonekura Y, Yamashita K, Saji H, Magata Y, Senda M, et al. Positron emission tomography using fluorine-18 deoxyglucose in evaluation of coronary artery bypass grafting. *Am J Cardiol* 1989; 64: 860–865.
7. Schelbert HR, Buxton D. Insights into coronary artery disease gained from metabolic imaging. *Circulation* 1988; 78: 496–505.
8. Nienaber CA, Brunken RC, Sherman CT, Yeatman LA, Gambhir SS, Krivokapich J, et al. Metabolic and functional recovery of ischemic human myocardium after coronary angioplasty. *J Am Coll Cardiol* 1991; 18: 966–978.
9. Marwick TH, MacIntyre WJ, Salcedo EE, Go RT, Saha G, Beachler A. Identification of ischemic and hibernating myocardium: feasibility of post-exercise F-18-deoxyglucose positron emission tomography. *Cathet Cardio-vasc Diagn* 1991; 22: 100–106.
10. Altehoefer C, Kaiser HJ, Doerr R, Feinendegen C, Beilin I, Uebis R, et al. Fluorine-18-deoxyglucose PET for assessment of viable myocardium in perfusion defects in technetium-99m MIBI SPECT: a comparative study in patients with coronary artery disease. *Eur J Nucl Med* 1992; 19: 334–342.
11. Altehoefer C, Vom Dahl J, Biedermann M, Uebis R, Beilin I, Sheehan F, et al. Significance of defect severity in technetium-99m-MIBI SPECT at rest to assess myocardial viability: comparison with fluorine-18-FDG PET. *J Nucl Med* 1994; 35: 569–574.
12. Snapper HJ, Shea NL, Konstam MA, Oates E, Udelson JE. Combined analysis of resting regional wall thickening and stress perfusion with electrocardiographic-gated technetium 99m-labeled sestamibi single-photon emission computed tomography: prediction of stress defect reversibility. *J Nucl Cardiol* 1997; 4: 3–10.
13. Kouris K, Clarke GA, Jarritt PH, Townsend CE, Thomas SN. Physical performance evaluation of the Toshiba GCA-9300A triple-headed system. *J Nucl Med* 1993; 34: 1778–1789.
14. Cuocolo A, Acampa W, Nicolai E, Pace L, Petretta M, Salvatore M. Quantitative thallium-201 and technetium-99m sestamibi tomography at rest in detection of myocardial viability in patients with chronic ischemic left ventricular dysfunction. *J Nucl Cardiol* 2000; 7: 8–15.
15. Udelson JE, Coleman PS, Metherall J, Pandian NG, Gomez AR, Griffith JL, et al. Predicting recovery of severe regional ventricular dysfunction: Comparison of resting scintigraphy with Tl-201 and Tc-99m-sestamibi. *Circulation* 1994; 89: 2552–2561.
16. Bodenheimer MM, Banka VS, Hermann GA, Trout RG, Pasdar H, Helfant RH. Reversible asynergy. Histopathologic and electrographic correlations in patients with coronary artery disease. *Circulation* 1976; 53: 792–796.
17. Ziffer JA, Cooke CD, Folks RD, LaPidus AS, Alazraki NP, Garcia EV. Quantitative myocardial thickening assessed with sestamibi: clinical evaluation of a count-based method. [abstract] *J Nucl Med* 1991; 32: 1006.
18. Chua T, Kiat H, Germano G, Maurer G, Van Train K, Friedman J, et al. Gated technetium-99m sestamibi for simultaneous assessment of stress myocardial perfusion, postexercise regional ventricular function and myocardial viability: correlation with echocardiography and rest thallium-201 scintigraphy. *J Am Coll Cardiol* 1994; 23: 1107–1114.
19. Williams KA, Taillon LA. Reversible ischemia in severe stress technetium99m-labeled sestamibi perfusion defects assessed from gated single-photon emission computed tomographic polar map Fourier analysis. *J Nucl Cardiol* 1995; 2: 199–206.

20. Marzullo P, Marcassa C, Sambuceti G, Parodi O, L'Abbate A. The clinical usefulness of electrocardiogram-gated Tc-99m methoxy-isobutyl-isonitrile images in the detection of basal wall motion abnormalities and reversibility of stress induced perfusion defects. *Int J Card Imaging* 1992; 8: 131–141.
21. Najm YC, Timmis AD, Maisey MN, Ellam SV, Mistry R, Curry PV, et al. The evaluation of ventricular function using gated myocardial imaging with ^{99m}Tc-MIBI. *Eur Heart J* 1989; 10: 142–148.
22. Tischler MD, Niggel JB, Battle RW, Fairbank JT, Brown KA. Validation of global and segmental left ventricular contractile function using gated planar technetium-99m-sestamibi myocardial perfusion imaging. *J Am Coll Cardiol* 1994; 23: 141–145.
23. Anagnostopoulos C, Gunning MG, Pennell DJ, Laney R, Proukakis H, Underwood SR. Regional myocardial motion and thickening assessed at rest by ECG-gated ^{99m}Tc-MIBI emission tomography and by magnetic resonance imaging. *Eur J Nucl Med* 1996; 23: 909–916.
24. Gunning MG, Anagnostopoulos C, Davies G, Forbat SM, Ell PJ, Underwood SR. Gated technetium-99m-tetrofosmin SPECT and cine MRI to assess left ventricular contraction. *J Nucl Med* 1997; 38: 438–442.
25. Stollfuss JC, Haas F, Matsunari I, Neverve J, Nekolla S, Schneider-Eicke J, et al. Regional myocardial wall thickening and global ejection fraction in patients with low angiographic left ventricular ejection fraction assessed by visual and quantitative resting ECG-gated ^{99m}Tc-tetrofosmin single-photon emission tomography and magnetic resonance imageing. *Eur J Nucl Med* 1998; 25: 522–530.
26. Rigo P, Leclercq B, Itti R, Lahiri A, Braat S. Technetium-99m-tetrofosmin myocardial imaging: a comparison with thallium-201 and angiography. *J Nucl Med* 1994; 35: 587–593.
27. Schwaiger M, Hicks R. The clinical role of metabolic imaging of the heart by positron emission tomography. *J Nucl Med* 1991; 32: 565–578.
28. Marshall RC, Tillisch JH, Phelps ME, Huang SC, Carson R, Henze E, et al. Identification and differentiation of resting myocardial ischemia and infarction in man with positron computed tomography, F-18-labeled fluorodeoxyglucose, and N-13 ammonia. *Circulation* 1983; 67: 766–778.
29. Brunken R, Schwaiger M, Grover-McKay M, Phelps ME, Tillisch J, Schelbert HR. Positron emission tomography detects tissue metabolic activity in myocardial segments with persistent thallium perfusion defects. *J Am Coll Cardiol* 1987; 10: 557–567.
30. Brunken RC, Kottou S, Nienaber CA, Schwaiger M, Ratib OM, Phelps ME, et al. PET detection of viable tissue in myocardial segments with persistent defects at Tl-201 SPECT. *Radiology* 1989; 172: 65–73.
31. Bonow RO, Dilsizian V, Cuocolo A, Bacharach SL. Identification of viable myocardium in patients with chronic coronary artery disease and left ventricular dysfunction. Comparison of thallium scintigraphy with reinjection and PET imaging with F-18 fluorodeoxyglucose. *Circulation* 1991; 83: 26–37.
32. Brunken R, Tillisch J, Schwaiger M, Child JS, Marshall R, Mandelkern M, et al. Regional perfusion, glucose metabolism, and wall motion in patients with chronic electrocardiographic Q wave infarction: Evidence for persistence of viable tissue in some infarct regions by positron emission tomography. *Circulation* 1986; 73: 951–963.
33. Tamaki N, Yonekura Y, Yamashita K, Senda M, Saji H, Hashimoto T, et al. Relation of left ventricular perfusion and wall motion with metabolic activity in persistent defects on thallium-201 tomography in healed myocardial infarction. *Am J Cardiol* 1988; 62: 202–208.
34. Fudo T, Kambara H, Hashimoto T, Hayashi M, Nohara R, Tamaki N, et al. F-18 deoxyglucose and stress N-13 ammonia positron emission tomography in anterior wall healed myocardial infarction. *Am J Cardiol* 1988; 61: 1191–1197.
35. Hoffman EJ, Huang SC, Phelps ME. Quantitation in positron emission computed tomography: 1. Effect of object size. *J Comput Assist Tomogr* 1979; 3: 299–308.
36. Fukuchi K, Uehara T, Morozumi T, Tsujimura E, Hasegawa S, Yutani K, et al. Quantification of systolic count increase in technetium-99m-MIBI gated myocardial SPECT. *J Nucl Med* 1997; 38: 1067–1073.
37. Sorenson JA, Phelps ME. *Physics in Nuclear Medicine*. Philadelphia; WB Saunders, 1987.
38. Matsunari I, Fujino S, Taki J, Senma J, Aoyama T, Wakasugi T, et al. Quantitative rest technetium-99m tetrofosmin imaging in predicting functional recovery after revascularization: Comparison with rest-redistribution thallium-201. *J Am Coll Cardiol* 1997; 29: 1226–1233.
39. Dilsizian V, Arrighi JA, Diodati JG, Quyyumi AA, Alavi K, Bacharach SL, et al. Myocardial viability in patients with chronic coronary artery disease. Comparison of ^{99m}Tc-sestamibi with thallium reinjection and [^{18}F]fluorodeoxyglucose. *Circulation* 1994; 89: 578–587.
40. Marzullo P, Sambuceti G, Parodi O. The role of sestamibi scintigraphy in the radioisotopic assessment of myocardial viability. *J Nucl Med* 1992; 33: 1925–1930.
41. DePuey EG, Rozanski A. Using gated technetium-99m-sestamibi SPECT to characterize fixed myocardial defects as infarct or artifact. *J Nucl Med* 1995; 36: 952–955.